

NASA/TM—2011-216986



Mach 0.3 Burner Rig Facility at the NASA Glenn Materials Research Laboratory

*Dennis S. Fox, Robert A. Miller, Dongming Zhu, and Michael Perez
Glenn Research Center, Cleveland, Ohio*

*Michael D. Cuy
ASRC Aerospace Corporation, Cleveland, Ohio*

*R. Craig Robinson
Jacobs Technology Inc., Cleveland, Ohio*

NASA STI Program . . . in Profile

Since its founding, NASA has been dedicated to the advancement of aeronautics and space science. The NASA Scientific and Technical Information (STI) program plays a key part in helping NASA maintain this important role.

The NASA STI Program operates under the auspices of the Agency Chief Information Officer. It collects, organizes, provides for archiving, and disseminates NASA's STI. The NASA STI program provides access to the NASA Aeronautics and Space Database and its public interface, the NASA Technical Reports Server, thus providing one of the largest collections of aeronautical and space science STI in the world. Results are published in both non-NASA channels and by NASA in the NASA STI Report Series, which includes the following report types:

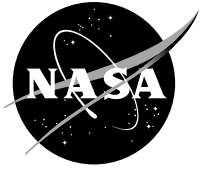
- **TECHNICAL PUBLICATION.** Reports of completed research or a major significant phase of research that present the results of NASA programs and include extensive data or theoretical analysis. Includes compilations of significant scientific and technical data and information deemed to be of continuing reference value. NASA counterpart of peer-reviewed formal professional papers but has less stringent limitations on manuscript length and extent of graphic presentations.
- **TECHNICAL MEMORANDUM.** Scientific and technical findings that are preliminary or of specialized interest, e.g., quick release reports, working papers, and bibliographies that contain minimal annotation. Does not contain extensive analysis.
- **CONTRACTOR REPORT.** Scientific and technical findings by NASA-sponsored contractors and grantees.

- **CONFERENCE PUBLICATION.** Collected papers from scientific and technical conferences, symposia, seminars, or other meetings sponsored or cosponsored by NASA.
- **SPECIAL PUBLICATION.** Scientific, technical, or historical information from NASA programs, projects, and missions, often concerned with subjects having substantial public interest.
- **TECHNICAL TRANSLATION.** English-language translations of foreign scientific and technical material pertinent to NASA's mission.

Specialized services also include creating custom thesauri, building customized databases, organizing and publishing research results.

For more information about the NASA STI program, see the following:

- Access the NASA STI program home page at <http://www.sti.nasa.gov>
- E-mail your question via the Internet to help@sti.nasa.gov
- Fax your question to the NASA STI Help Desk at 443-757-5803
- Telephone the NASA STI Help Desk at 443-757-5802
- Write to:
NASA Center for AeroSpace Information (CASI)
7115 Standard Drive
Hanover, MD 21076-1320



Mach 0.3 Burner Rig Facility at the NASA Glenn Materials Research Laboratory

*Dennis S. Fox, Robert A. Miller, Dongming Zhu, and Michael Perez
Glenn Research Center, Cleveland, Ohio*

*Michael D. Cuy
ASRC Aerospace Corporation, Cleveland, Ohio*

*R. Craig Robinson
Jacobs Technology Inc., Cleveland, Ohio*

National Aeronautics and
Space Administration

Glenn Research Center
Cleveland, Ohio 44135

Acknowledgments

The authors would like to acknowledge the efforts of others that provided key contributions to the facility throughout its history: Carl A. Stearns, James (Jimmy) R. Johnston, Thomas Schneider, Dennis L. Weismantel, Steve DeBarr, Richard D. Rinehart, R. Craig Robinson, Robert T. Pastel, Ruben J. Ramos, Eric W. Sockel, Daniel L. Deadmore, Carl E. Lowell, Richard L. Ashbrook, and Leonard J. Bunyai.

This work was sponsored by the Fundamental Aeronautics Program
at the NASA Glenn Research Center.

Level of Review: This material has been technically reviewed by technical management.

Available from

NASA Center for Aerospace Information
7115 Standard Drive
Hanover, MD 21076-1320

National Technical Information Service
5301 Shawnee Road
Alexandria, VA 22312

Available electronically at <http://www.sti.nasa.gov>

Mach 0.3 Burner Rig Facility at the NASA Glenn Materials Research Laboratory

Dennis S. Fox, Robert A. Miller, Dongming Zhu, and Michael Perez
National Aeronautics and Space Administration
Glenn Research Center
Cleveland, Ohio 44135

Michael D. Cuy
ASRC Aerospace Corporation
Cleveland, Ohio 44135

R. Craig Robinson
Jacobs Technology Inc.
Cleveland, Ohio 44135

Abstract

This Technical Memorandum presents the current capabilities of the state-of-the-art Mach 0.3 Burner Rig Facility. It is used for materials research including oxidation, corrosion, erosion, and impact. Consisting of seven computer controlled jet-fueled combustors in individual test cells, these relatively small rigs burn just 2 to 3 gal of jet fuel per hour. The rigs are used as an efficient means of subjecting potential aircraft engine/airframe advanced materials to the high temperatures, high velocities and thermal cycling closely approximating actual operating environments. Materials of various geometries and compositions can be evaluated at temperatures from 700 to 2400 °F (370 to 1316 °C). Tests are conducted not only on bare superalloys and ceramics, but also to study the behavior and durability of protective coatings applied to those materials.

1.0 Introduction

The state-of-the-art Mach 0.3 Burner Rig Facility is located within the Materials Research Laboratory (MRL, building 34) at the National Aeronautics and Space Administration's Glenn Research Center (GRC). It is used for materials research including oxidation, corrosion, erosion, and impact. Consisting of seven computer controlled jet-fueled combustors in individual test cells, these relatively small rigs burn just 2 to 3 gal of jet fuel per hour. The name of the facility comes from the velocity of the exhaust gas stream (~335 ft/sec, or ~102 m/s). The rigs are used as an efficient means of subjecting potential aircraft engine/airframe advanced materials to the high temperatures, high velocities and thermal cycling closely approximating actual operating environments. Materials of various geometries and compositions can be evaluated at temperatures from 700 to 2400 °F (370 to 1316 °C). In addition, materials can be subjected to thermal cycling, which duplicates the flight cycles experienced by aircraft making daily takeoffs and landings. This facility is primarily used in test programs for NASA Fundamental Aeronautics Programs. Additional research has been conducted with aircraft gas turbine engine companies including General Electric Aviation, Pratt & Whitney, Rolls-Royce, LibertyWorks (formerly Allison Advanced Development Co.), Honeywell Aerospace (formerly AlliedSignal Engines) and Williams International; the United States Air Force, Navy and Army; various material suppliers; other NASA field centers; and academia.

The primary focus of this Technical Memorandum is to present the *current* capabilities of the facility. The backbone of each facility—the burner itself—is constant throughout the facility. However, the materials test configuration is unique in each test cell. Current capabilities include cyclic oxidation

(hot-cold, or idle-takeoff-cruise), corrosion, erosion, impact, and tensile loading. Tests are conducted not only on bare superalloys and ceramics, but also to study the behavior and durability of protective coatings applied to those materials.

The secondary focus of this memorandum is to document past studies conducted in the facility, primarily through an extensive listing of papers in the bibliography. The Appendix summarizes the work conducted using more unique NASA GRC burner rigs. The high pressure burner rig is still in operation, while the 4-atmosphere corrosion rig and Mach 1 rig have been dismantled. Finally, some archival photos are presented. The Mach 0.3 burner rig facility is located within the Durability & Protective Coatings Branch: <http://www.grc.nasa.gov/WWW/StructuresMaterials/DPC/>, part of the Structures & Materials Division: <http://www.grc.nasa.gov/WWW/StructuresMaterials/>, in the Research and Technology Directorate: <http://rt.grc.nasa.gov/>.

2.0 Description and Operation of Mach 0.3 Burner Rig

A schematic representation of a standard Mach 0.3 burner rig is presented in Figure 1. Note that the standard exhaust nozzle diameter is 1 in. (2.5 cm) in diameter, though other nozzles have been used previously. A detailed description of burner operation is found in References 1 and 2, and it is summarized here. Maximum sample temperature that can be achieved on a single fixed sample is nominally 2400 °F (1316 °C). Each rig utilizes 120 psig (800 kPa) filtered shop air supplied via the GRC central air system. Air flow is measured with Sponsler (Lake Bluff, IL) type 2503 turbine flow meters (electronic output to computer) and Fisher & Porter (Warminster, PA) Precision Bore rotometers (visual float-type air flow indication on rig). To run at Mach 0.3 approximately 2.5 lb/min airflow is used. For higher Mach numbers up to 7.0 lb/min airflow is available. Air is preheated to 500 °F (260 °C) to

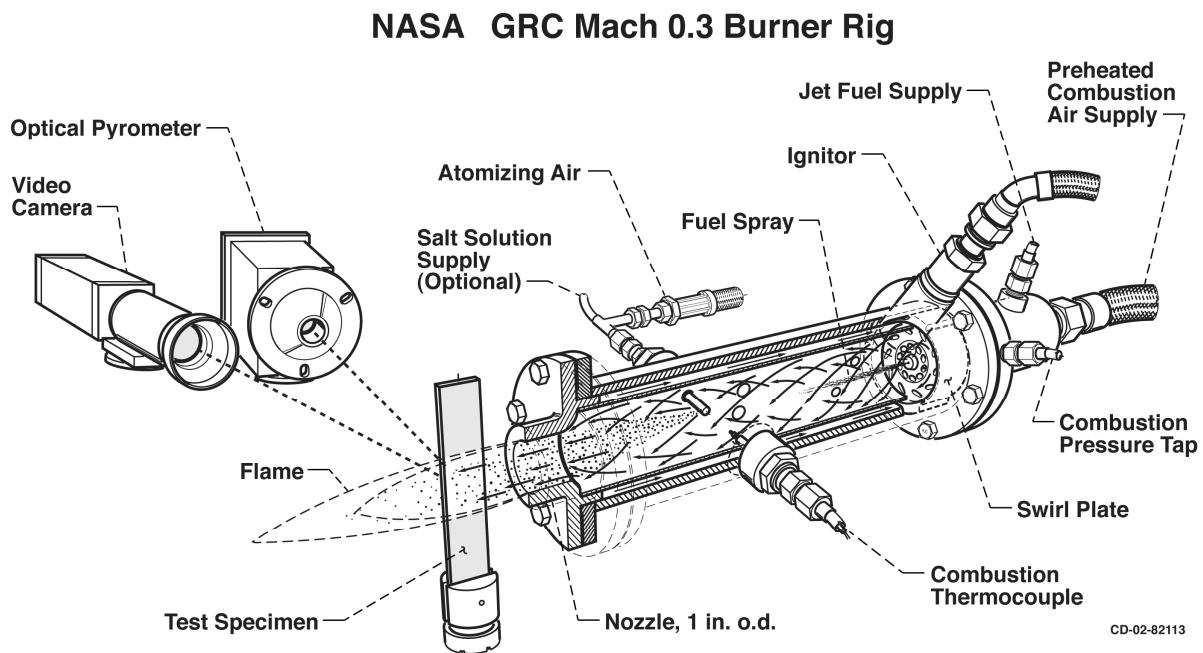


Figure 1.—Mach 0.3 burner rig cross-sectional schematic.

minimize coking within the combustor can, and it is delivered through a 0.75 in. (1.9 cm) diameter line and forced through a co-rotating swirl plate. Jet fuel is provided from a 5000 gal (19,000 liter) underground storage tank. A low pressure fuel pump (35 psig) delivers filtered fuel to the building. A high pressure pump (350 psig) then delivers fuel to each test cell, where it is injected into the combustor using off-the-shelf Goodrich-Delavan oil burner fuel nozzles located in the center of the swirl plate. The most commonly used fuel nozzle delivers 1.5 gph, with others on-hand ranging from 0.5 to 3.5 gph. Type “A” nozzles have a solid cone of spray particles, whereas Type B’s spray pattern is only located on the perimeter of the cone. The nozzles come in cone spray patterns from 45° to 80°, with an 80° “hollow” Type “B” cone providing the best overall combustion performance (e.g., soot-free flame, minimal coking of the combustor can).

Pressure within the combustor is measured with a transducer, and is usually held 1 psi above ambient. This ΔP determines the Mach 0.3 flame velocity. An aircraft-type igniter initiates combustion. The inner liner is made of Inconel 601 superalloy, with its outer diameter cooled with bypass air. Downstream this air is added to the combustion process through liner perforations. A Type “K” thermocouple is used to confirm the presence of a flame. For corrosion studies, an optional salt-solution injector can be used. Sample temperature can be measured in a variety of ways. Routinely, an optical pyrometer is used as illustrated in Figures 1 and 2. Another monitoring technique is the use of a video camera recording system. Since the rigs are employed around-the-clock, video can be used to capture certain events occurring outside of first shift, such as spallation of a thermal barrier coating. There are currently seven burner rigs in the facility, each housed separately in a test cell that has a 10 by 10 ft (3 by 3 m) footprint and is 12 ft (~3.7 m) high.



Figure 2.—Mach 0.3 burner used in thermal blanket durability study. (NASA photo C-1994-5005, November 1994, from Ref. 33).

The Mach 0.3 burners at GRC are based on a Pratt & Whitney (East Hartford, CT) design. The earliest ones came on line in the early 1970s. At first, the rigs were operated in a constantly attended mode. With the advent of personal computers (PCs) in the early 1980s, digital control of the burner rigs became viable. This made them highly flexible and provided accurate means of 24/7 unattended material durability testing. A Technical Memorandum (TM) containing detailed information of both Mach 0.3 burner hardware and the first version of digital temperature and velocity control (including computer code) was published in 1985 (Ref. 2). Figure 3 is a simple schematic diagram of the burner rig control system hardware from that paper. The Mach 0.3 Burner Rig Operator's Manual (Ref. 3) was published in 1987, and Figure 4 is a promotional viewgraph with both authors pictured.

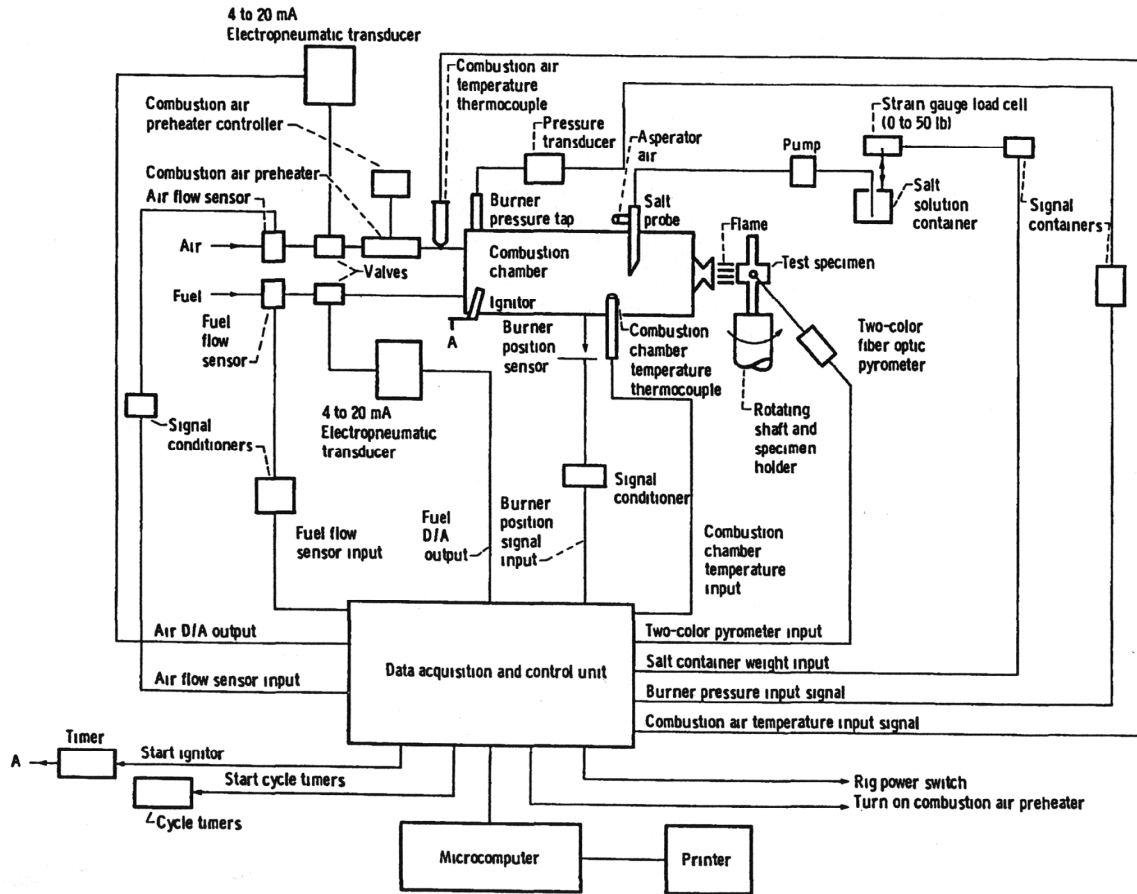


Figure 3.—Schematic diagram of the burner rig control system hardware (from Ref. 3).

MACH 0.3 BURNER RIG FOR ENVIRONMENTAL DURABILITY OF ADVANCED MATERIALS

EFFICIENT MEANS OF SUBJECTING POTENTIAL AIRCRAFT ENGINE/AIRFRAME MATERIALS TO HIGH TEMPERATURE, HIGH VELOCITY, AND THERMAL CYCLING, CLOSELY APPROXIMATING THE ACTUAL OPERATING ENVIRONMENT



OPERATING PARAMETERS

**MODES: OXIDATION OR CORROSION
(SALT-SEEDED FLAME)**
FUEL: JET A, DIESEL
FLAME VELOCITY: MACH 0.2-0.5
PRESSURE: ATMOSPHERIC
SAMPLE TEMPERATURE: 700-2500 °F
THERMAL CYCLING CAPABILITIES:
 SEQUENTIAL, INTERMEDIATE
 MULTIPLE TEMP. PROFILE CYCLES
**SAMPLES MAY BE ROTATED OR
 HELD STATIONARY**
**COMPATIBLE WITH WIDE RANGE
 OF SAMPLE GEOMETRIES**

CD-87-30248

Figure 4.—Promotional viewgraph (circa 1987) for the PC controlled burner rigs. Note the IBM PC with two 5.25 in. floppy disk drives. Reference 3 authors shown.

The computer control system used today was installed in 1987. As of this writing, antiquated but rugged 486-based machines are still used to run a DOS-based program with version 1.1 installed in July of 1987. The control system is a hybrid—both computer (digital) and electromechanical (analog). Via a suitable interface, the PC acquires specimen temperature (usually via an optical pyrometer), fuel pressure, fuel flow, burner can pressure, and other rig parameters. Specimen temperature is then controlled by digital adjustment of fuel flow using a PID control algorithm. Also included in the computer control functions are safety features such as emergency shutdowns, test condition measurements, record keeping of test data, display of testing status, and mathematical calculations.

Five different test modes can be selected when starting each test:

1. Pyrometer/Fuel—This mode is used the majority of the time. It maintains a specific sample surface temperature (± 6 °C/ ± 10 °F), as measured with the pyrometer, by adjusting fuel flow.
2. Fuel/Air ratio—This mode maintains a specific fuel-to-air ratio throughout the test, with regard to the desired temperature of a thermocoupled dummy sample. The software adjusts temperature of the dummy (minimum 60 sec needed) and then pivots the burner onto the actual sample.
3. Thermocouple/Fuel—This mode maintains a specific sample temperature (± 6 °C/ ± 10 °F; sample is thermocoupled) by adjusting fuel flow.
4. Thermocouple/Air—In this mode, the temperature of a hollow thermocoupled specimen is held steady by adjusting cooling air flow through the sample. A preselected fuel-to-air ratio is maintained throughout the test.
5. Pyrometer/Air—In this mode, the temperature of a hollow specimen as measured with an optical pyrometer is held steady by adjusting cooling air flow through the sample. A preselected fuel-to-air ratio is maintained throughout the test.



Figure 5.—Top left: Assortment of carousels used for cylindrical, rectangular, and occasional odd-shaped samples (such as those in Fig. 20). Top right: Cylindrical sintered α -silicon carbide samples in test carousel (NASA GRC photo C-1991-10893). Bottom: Superalloy sheets in carousel test (C-1999-2482).

Another test mode choice is that of thermal cycling, wherein the burner can be pivoted on-and-off the sample a specified number of times. Also, forced air cooling can be applied to the specimen when the burner is pivoted off of the sample(s). Single samples are fixed in place and impinged on by the flame, with the impingement angle specified by the customer. If a number of specimens are to be tested, a spinning sample carousel (100 to 200 rpm) is utilized (see Fig. 5). Carousels are fabricated in-house according to customer needs. It should be noted that a single specimen can also be rotated in the flame, if desired.

In Figure 6 are photographs of the Mach 0.3 burner rig facility control room and one of the test cells.



Figure 6.—Top: Mach 0.3 burner rig facility control room. Each of the seven rigs is housed in individual test cells behind the operator as he sits.
Bottom: Looking through the soundproof door into one of the test cells.

3.0 Current Research and Specific Test Cell Configurations

3.1 3 by 3 in. Plate Oxidation

Superalloys are metals used at high temperatures in the hot sections of gas turbine engines. This class of material retains significant strength to temperatures near 1830 °F (1000 °C). An understanding of the oxidation and hot corrosion behavior of superalloys is of great importance. In this demanding application, components such as turbine blades and vanes are often protected with Thermal Barrier Coatings (TBCs). These thin 5 to 10 mil (0.125 to 0.25 mm) zirconia-based ceramic coatings, when coupled with internal air cooling, allow the components to be operated at temperatures 100 to 200 °F higher than bare components.

In this test cell, square oxidation samples (coated or uncoated) are held at a 45° angle to the flow direction and held in a superalloy “picture frame.” The burner is fixed in place (doesn’t pivot). Via electromechanical actuation, the sample can be moved close to the 1 in. diameter burner exit nozzle to model the high temperatures encountered during full power engine conditions such as takeoff, far from the nozzle to mimic engine idle conditions, and to an intermediate position to model cruise conditions. The sample can be rapidly translated (within seconds) from 1 to 18 in. away from the burner nozzle. Some customers specify up to three positions, with the corresponding temperatures at those positions relating to idle, cruise and takeoff/landing conditions. Preferred sample size is 3 by 3 in. (7.6 by 7.6 cm) as shown in Figure 7, though 2 by 2 in. (5 by 5 cm) and 4 by 4 in. (10.2 by 10.2 cm) samples have also been tested.



Figure 7.—Durability testing of a 3 by 3 in. superalloy plate protected with a thermal barrier coating.

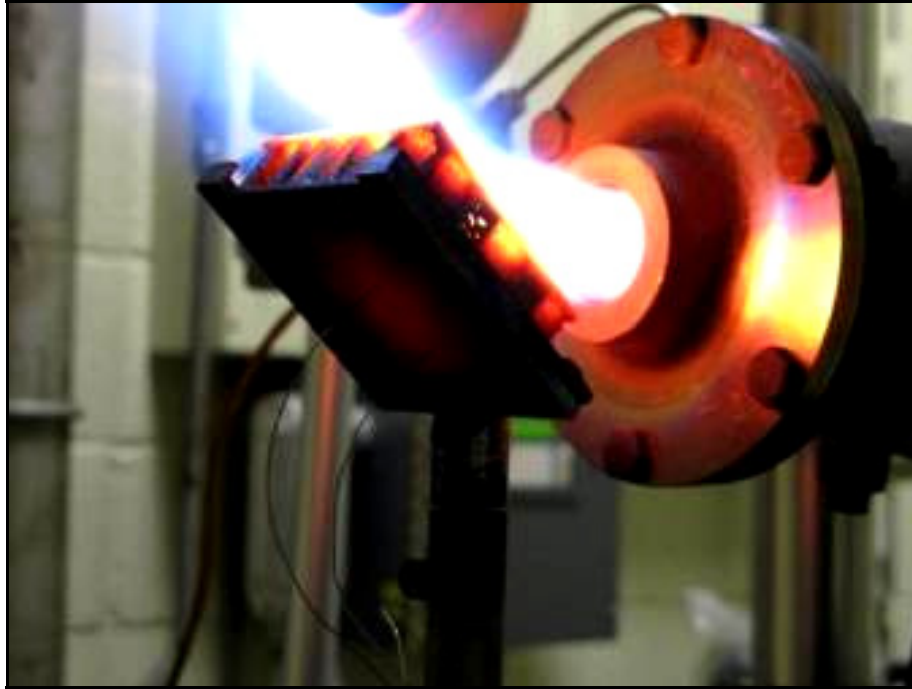


Figure 8.—Exposure of a 2 by 2 in. carbon fiber reinforced silicon carbide matrix composite “sandwich” to a top face temperature of 2300 °F. Heat transfer across the panel is measured using an optical pyrometer on the top face and two Type “K” thermocouples on the back face.

Ceramics such as silicon carbide and silicon nitride are generally stable to higher temperatures than most metals and alloys. These materials form a stable film of silica (SiO_2) in an oxidizing environment. The development of high temperature structural ceramics for advanced gas turbine engines has been an area of active research for many years. In such applications, ceramics are exposed not only to high temperatures but also aggressive gases (including water vapor) and possibly deposits (sea salt). Water vapor attack of the silica scale results in parabolic oxidation and recession of the substrate at unacceptable rates. Environmental Barrier Coatings (EBCs) have been developed to address this problem. In the case of sea salt hot corrosion, the concern of corrosion is loss of load bearing capability due to pitting of the surface. Oxidation studies of silicon-based ceramics are also conducted with this plate oxidation rig, an example shown in Figure 8.

3.2 Corrosion

Hot corrosion is an accelerated attack experienced by superalloys and silicon-based ceramics that is initiated by the deposition of condensed sodium sulfate (Na_2SO_4) on engine parts. The source of the salt is direct ingestion with intake air or by its formation during combustion from sodium chloride-contaminated air and sulfur in the fuel. Most superalloys/ceramics are susceptible to hot-corrosion attack to some extent. The phenomenon depends on many factors, including temperature, cyclic conditions, material composition, impurities in and pressure of air ingested into the engine, and impurities in the fuel. In this test, samples are normally held in a sample carousel. The one illustrated in Figures 9 and 10 holds 18 superalloy pins nominally 0.25 in. diameter by 3 in. tall (0.64 cm diameter by 7.6 cm tall). A synthetic sea salt solution (mixed in-house) is pumped through an air atomizer and injected into the combustion can as shown in the Figure 1 schematic. Solutions in the 0.1 to 10 parts-per-million range have been used; higher concentrations tend to clog the atomizer.



Figure 9.—Carousel holding eighteen specimens, each 1/4 diameter by 3 in. tall. Samples were undergoing synthetic sea salt corrosion to determine the effectiveness of protective metallic coatings.



Figure 10.—Results of the above 900 °C (1650 °F), 500 hr corrosion test with 8 ppm synthetic sea salt. The most corrosion resistant samples are located at the forefront.

3.3 Impact Gun and TBC Particle Impact

A gas turbine engine ingests enormous amounts of air. At the same time, it can also suck in foreign objects such as dust, dirt, volcanic ash, sand, rocks, ice, hail, and man-made objects (e.g., nuts, bolts). This can cause foreign object damage (FOD), a problem so severe that a technical society is devoted to the issue (National Aerospace FOD Prevention, Inc., <http://www.fodnews.com/>). An impact gun based on a small particle gun first developed in the Ballistic Impact Laboratory (<http://rt.grc.nasa.gov/main/rlc/ballistic-impact-laboratory/>) is used to fire 1/16 in. diameter steel balls at samples heated by the burner rig (Figs. 11 and 12). Velocities range from 50 m/sec to a maximum of 400 m/sec. Studies of the impact resistance of both uncoated and environmental barrier coated SiC/SiC composites using the small particle gun are found in References 40 and 41.



Figure 11.—Top: The small cylinder is filled with helium from the “K” bottle, and the “Red Hat” valve is actuated to accelerate the round projectile toward the sample down a hypodermic metal tube (1/16 in. ID) inserted in a larger diameter (1/8 in. ID) stainless steel barrel. Bottom: Business end of impact gun. Exit of barrel is protected from the flame with ceramic insulation. In this case, a superalloy target sample is held in a “C” clamp arrangement.



Figure 12.—Uncoated CMC tensile “dogbone” specimens (6 by 1/2 by 1/8 in.) after impact with a 1/16 in. diameter steel ball bearing at various temperatures and projectile velocities.

Aircraft gas turbine engines are subject to damage from *erosion* (generally caused by particles tens of microns in diameter) or *impact* damage (generally from particles hundreds of microns in diameter). This rig is also being modified to allow another type of impact testing, similar to the rig discussed in Section 3.4. The impact gun will be temporarily moved, and 560 μm particles will be added to the combustor can to model particle *impact* (as opposed to erosion) of TBC coated specimens. In the rig described in the next Section 3.4 smaller 50 to 100 μm alumina grit is added to the combustor can for TBC *erosion* studies that model sand ingestion by helicopter turbine engines.

3.4 Erosion

Considerable advances in engine performance are required over the next several decades. Advanced TBCs will be an important part of all future gas turbine engines. As stated in the previous section, aircraft gas turbine engines are subject to ingested dirt/dust/sand damage from erosion (generally caused by particles tens of microns in diameter) or impact damage (generally from particles hundreds of microns in diameter). Particulate ingestion may be more severe at low altitudes, from hovering of rotorcraft during takeoff and landing, and from operation under harsh conditions. The shedding of particles from the combustor is another important source of particulate matter. Unless future TBCs are erosion resistant, coating loss from erosion and impact damage will be a factor limiting future advancements. Reference 4 describes current turbine blade TBC development at GRC, as well as the study of the coating’s impact and erosion resistance validated in laboratory-simulated engine erosion and/or thermal gradient environments using the unique Mach 0.3 burner rig described here.

A standard Mach 0.3 burner rig was modified to allow Mach 0.3 to 1.0 velocities and erosion capabilities to study advanced turbine blade TBCs in a simulated turbine engine-relevant erosion environment (Figs. 13 to 15). Rig development emphasized increasing the erodent particle velocities at high temperatures by increased gas mass flow rate, erodent flow uniformity with improved feeding systems, and relevant thermal gradients found in turbine environments. The high velocity burner erosion rig includes a 1.9 mm (3/4 in.) diameter highly efficient burner nozzle, a specimen holder fixture and precision erodent feeder.

The burner nozzle inner surface contour was designed based on an ANSI/ASME nozzle standard to achieve better flame stability and uniformity, with the overall configuration modified to accommodate increased burner mass flow and higher heat flux environments. The nozzle was made of a single crystal nickel-base superalloy turbine blade material to ensure high temperature durability.

To achieve high erosion particle velocities, a computational fluid dynamics modeling (CFD) approach in conjunction with experimental investigations was employed to optimize the burner and erodent injection design. The CFD model (Fluent/ANSYS; Canonsburg, PA) was used to calculate the gas and particle velocities for the burner rig temperatures and pressures of interest. The modeling and experimental testing were conducted in relevant burner velocities ranging from Mach 0.3 to 0.9, representative of turbine engine conditions. Alumina (Al_2O_3) particles were used as the erodent and nominal particle sizes ranged from 27 to 560 μm in order to understand the broad coating erosion and impact behavior.

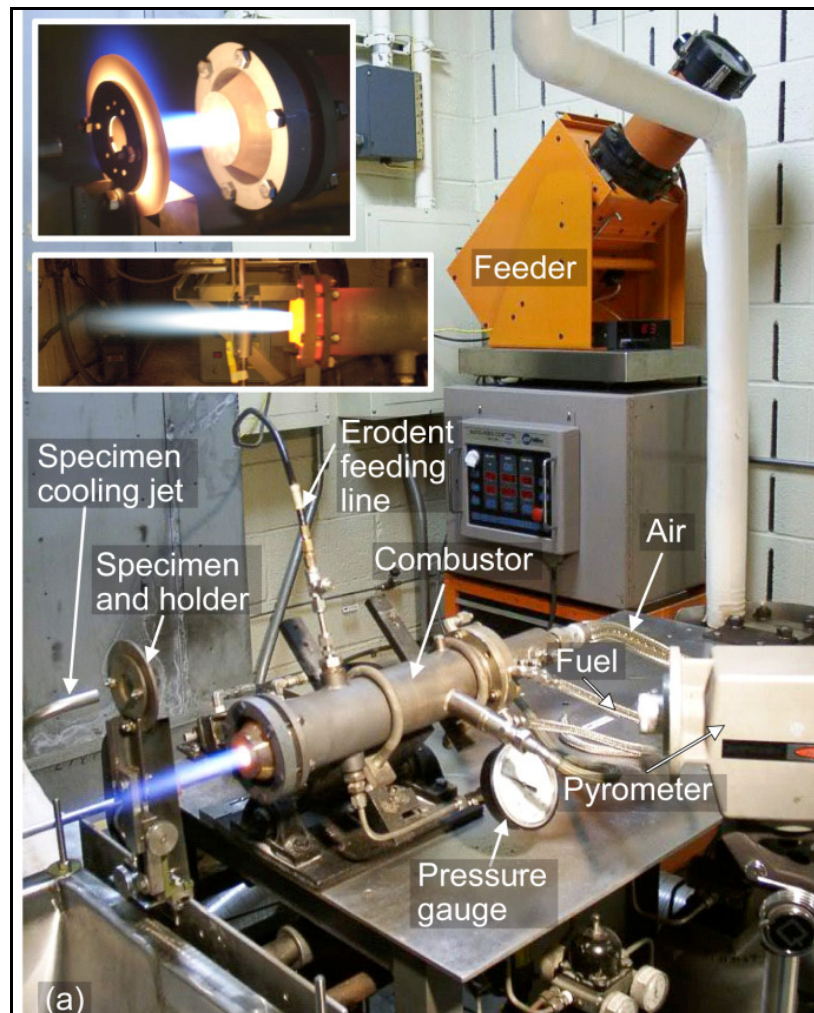


Figure 13.—Modified burner rig for Mach 0.3 to 1.0 erosion testing. The dust collection system is not shown.

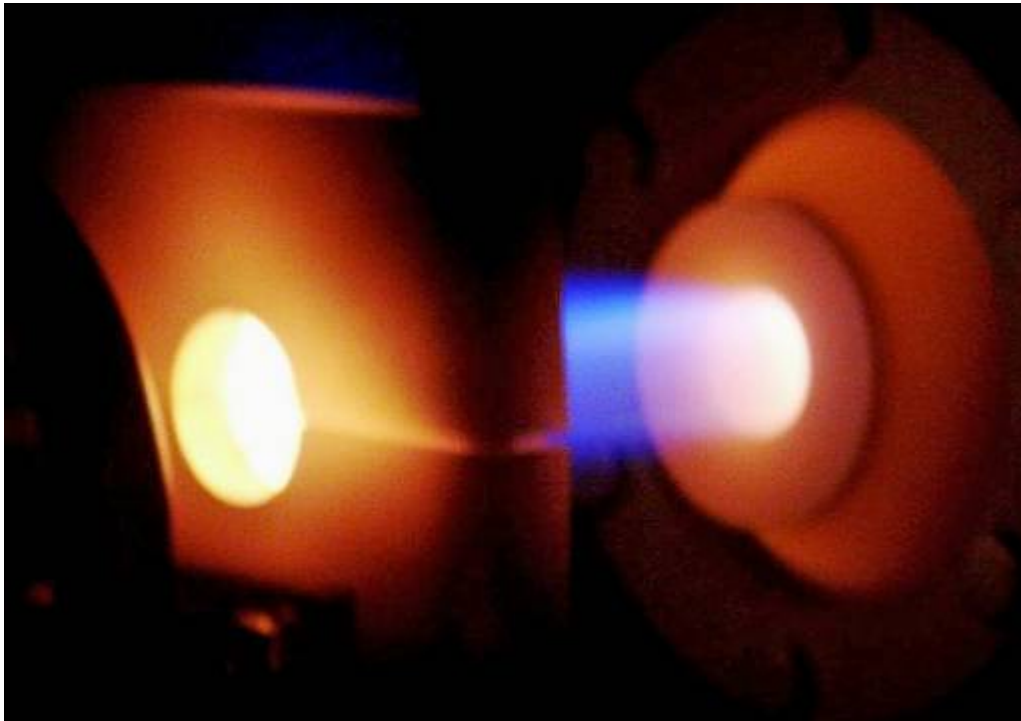


Figure 14.—2.5 cm diameter sample (in clamshell holder) exposed to erosion rig burner exhaust nozzle operating at Mach 0.5.

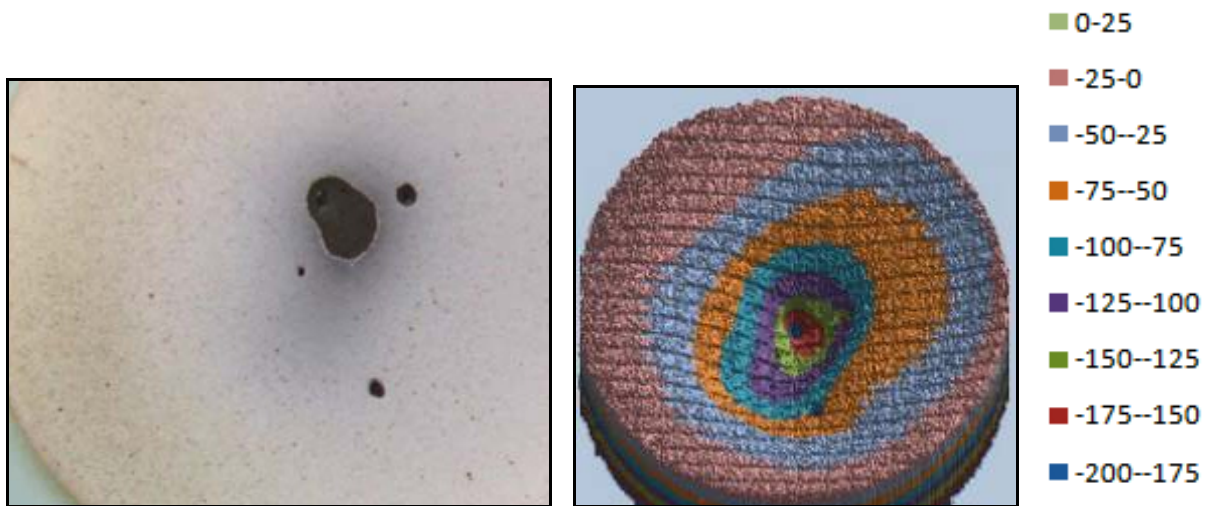


Figure 15.—Left: 2.5 cm diameter superalloy button with improved TBC after erosion testing; Right: Digital image of eroded specimen and corresponding micron scale from contour tracer (Zygo, Middlefield, CT) illustrating penetration depth.

A modified burner rig configuration with an extension duct (300 mm in length and 19 mm inner diameter) was explored to further accelerate the erodent particle and increase the velocity using 50 and 560 μm size Al_2O_3 particles. Erosion rates are determined by interrupted coating erosion thickness recession and weight-loss measurements, and also by the amount of erodent required for penetration of the coating to expose the substrate. In Reference 4 the coating erosion evaluations was primarily conducted at 1800 and 2000 °F (coating surface \sim 1900 and \sim 2100 °F, respectively) using 27 μm size Al_2O_3 particles, with additional tests conducted at 2200 °F.

3.5 Tensile Loading

In combustion environments, silicon-based ceramics are prone to enhanced recession due to the reaction of its protective silica (SiO_2) scale with water vapor to form gaseous $\text{Si}(\text{OH})_4$. Environmental barrier coatings (EBCs) were developed to protect Si-based Ceramic Matrix Composites (CMCs) from such attack. This Mach 0.3 burner rig test cell contains a very simple mechanical test frame (Fig. 16) used to apply tensile loads primarily to ceramic matrix composites (bare or coated). Imposed crack formation allows penetration of the combustion gases to the substrate, allowing oxidation of the reinforcing fiber and interphase to occur. Metal samples have been tested in this rig as well. A very unique material studied in this rig was an Inconel 718 Lattice Block Structure.

3.6 Thermal Barrier Coating Durability

Life prediction studies of TBCs and their metallic bond coats - primarily as applied to solid superalloy rods - have been conducted in the past. These insulating coatings thermally protect components and allow higher operating temperatures. At the same time, component life is extended by reductions in oxidation and thermal fatigue. In conjunction with active film cooling, TBCs permit working temperatures higher than the melting point of the metal blade/vane. TBCs are applied to the superalloy substrate using the plasma spray technique. A powder such as zirconia is introduced into a plasma jet emanating from a torch, the temperature of which is on the order of 5000 °F. The zirconia powder melts and is propelled towards a substrate, wherein molten droplets of the ceramic solidify to develop the desired coating. There are a large number of variables in this technique including powder type/size, powder manufacturer, plasma gas composition, gas flow rates, energy input, standoff distance from the torch to the substrate, and powder deposition rate. The life of the coating is a function of all of these variables, and the burner rig is an excellent tool to conduct lifing studies.

Exposure of single rotating specimens can be conducted (Fig. 17), but a higher amount of sample throughput is achieved using an eight-place sample carousel (Fig. 18). Samples can be exposed for hundreds of hours of unattended thermal cycling. A video camera with time stamping can be triggered to take \sim 30 sec of video every time the burner pivoted on the sample set. A TBC delamination appears as a hot spot, and the rig operator can use the videotape to determine time of failure. The failed specimen can be replaced with a new specimen, and the carousel test continued.

The application of thick thermal barrier coatings (TTBCs) to low heat rejection diesel engine combustion chambers was a subject of study in the early 1990s by companies such as Caterpillar (Peoria, IL) and Cummins Engine Company, Inc., (Columbus, IN). Areas of TTBC technology examined at the time included powder characteristics and chemistry; bond coat composition; coating design, microstructure and thickness as they affect properties, durability, and reliability; and TTBC “aging” effects (microstructural and property changes) under diesel engine operating conditions (Ref. 43). Figure 19 is a photo of burner rig testing of such coatings, circa 1997.

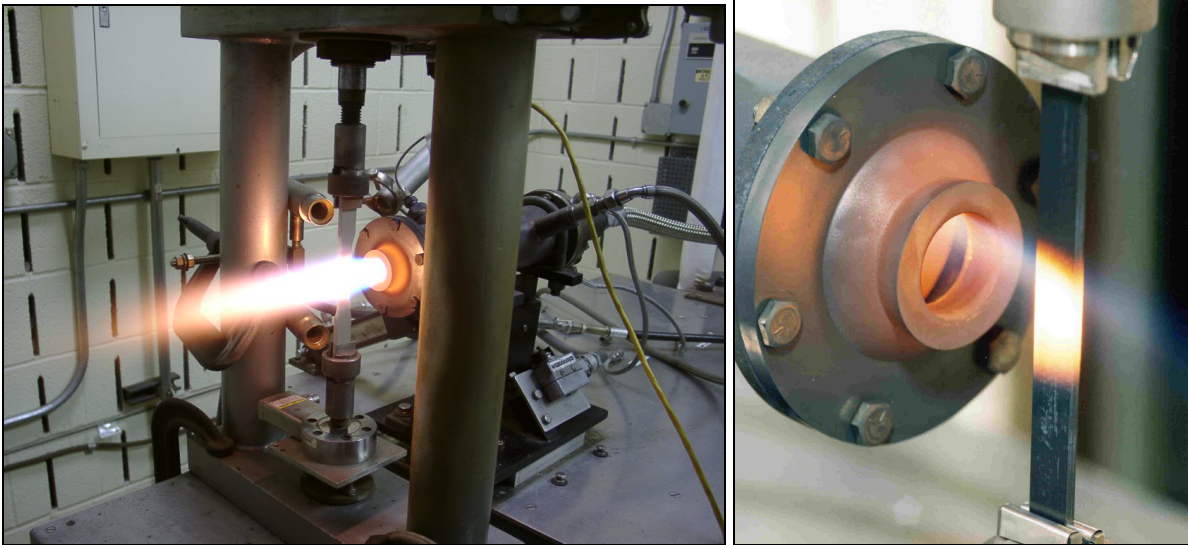


Figure 16.—Tensile test in conjunction with burner rig exposure. Left, coated CMC tensile “dogbone” specimen. Right, uncoated Si-based CMC.

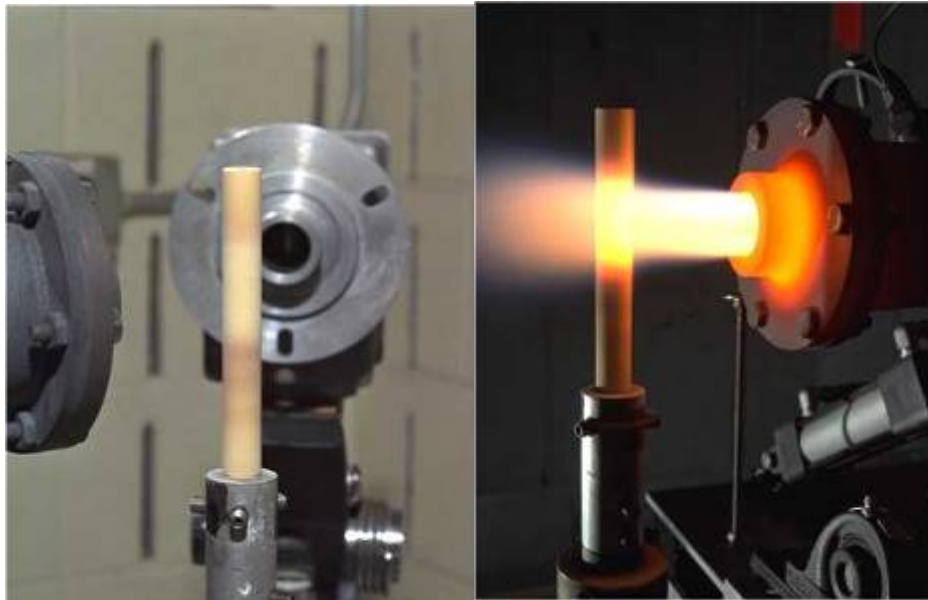


Figure 17.—Burner rig exposure of a single spinning thermal barrier coated superalloy. Nominal sample size of solid rod: 1/2 in. diameter, 5 in. tall. GRC photo numbers C-1999-2485 and C-1999-2487.



Figure 18.—Eight place carousel for burner rig exposure of a multiple thermal barrier coated superalloy specimens. Nominal size of coated solid rod: 1/2 in. diameter, 5 in. tall.

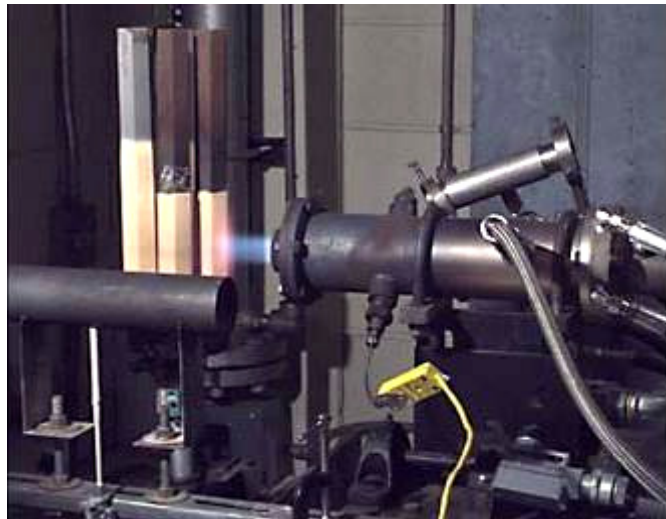


Figure 19.—Burner rig exposure of diesel thermal barrier coatings (NASA photo C-1997-2825).

4.0 Historic NASA Aeronautics Program Research

As noted, the main customers of the facility are the fundamental NASA aeronautics programs. In the mid 1990's as part of the Enabling Propulsion Materials Program, it was used to support Task B – Exhaust Nozzle. The objective of this task was to provide the necessary material technology required for an economically viable and environmentally acceptable High Speed Civil Transport HSCT exhaust system (Ref. 33). Mach 0.3 burner rig tests were performed to evaluate the insulating capability of the thermal protection system, or TPS (see Fig. 2). After exposure, the samples were examined for any physical degradation, such as loss of flexibility or mechanical integrity.

As part of the General Aviation Program in the late 1990s, the oxidation and corrosion of turbine engine blades and vanes manufactured by Williams International for the lightweight FJX-2 turbofan engine was studied (see Fig. 20). The testing was cyclic in nature, with each cycle consisting of 60 min in the flame and 10 min with the burner pivoted off the sample. Also, parts-per-million amounts of a synthetic sea salt solution were injected into the burner can for the first few minutes of the 1-hr hot cycle. This engine was to power General Aviation Program's V-Jet demonstrator test bed aircraft. A description of the program is found here: [http://www.docstoc.com/docs/1084022/The-General-Aviation-Propulsion-\(GAP\)-Program](http://www.docstoc.com/docs/1084022/The-General-Aviation-Propulsion-(GAP)-Program).

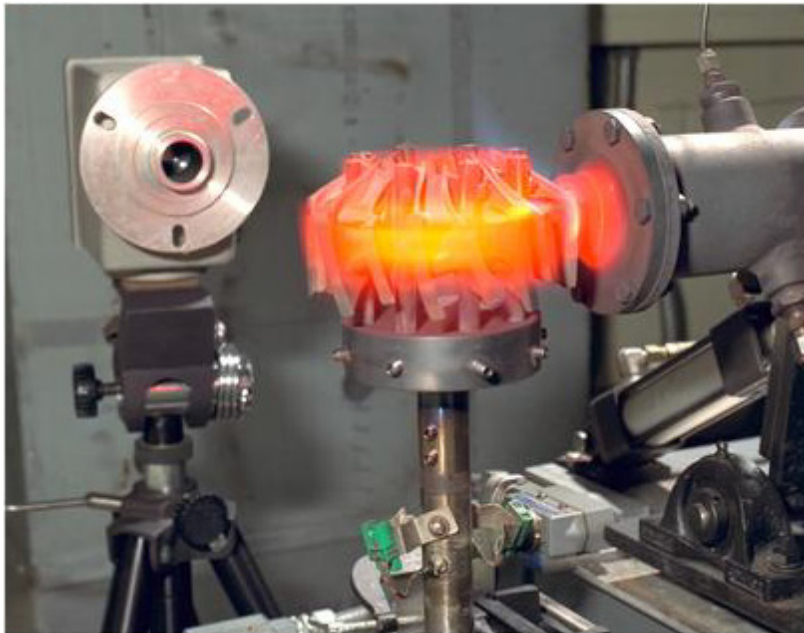


Figure 20.—Oxidation tests of engine vanes for General Aviation Propulsion Program (NASA photo C-28-270).

Appendix—Other Unique NASA GRC Burner Rigs

The High Pressure Burner Rig (HPBR) is currently housed in the Special Projects Laboratory (building 24) and is a combustion test rig used for high-temperature environmental durability studies of materials for advanced aircraft (Fig. 21). The facility burns jet fuel and air in controlled ratios to produce combustion gas chemistries and temperatures that are similar to those in gas turbine engines. In addition, the test section is also capable of simulating the pressures and gas velocities representative of today's aircraft. A brief summary is given here, with a detailed test facility description and history of development is found in References 44 and 45 are summarized here.

The HPBR typically operates with a fuel-lean gas mixture. However, with the proper scrubber and waste disposal systems, the facility can also be operated using fuel-rich gas mixtures. Test samples are easily accessible for ongoing inspection and documentation of weight change, thickness, cracking, and other metrics. Temperature measurements are available in the form of both Types "B" and "R" thermocouples as well as 2-color and 8 μm optical pyrometers. The facility is also equipped with quartz windows for observation and videotaping. The facility has a wide range of operating conditions including: up to 2.0 lbm/sec airflow (combustion and/or secondary cooling); equivalence ratios 0.5 to 1.0 (lean-burn); gas temperatures of 1500 to 3000 °F; test pressure range of 4 to 12 atmospheres; and gas flow velocities of 30 to 100 ft/sec.

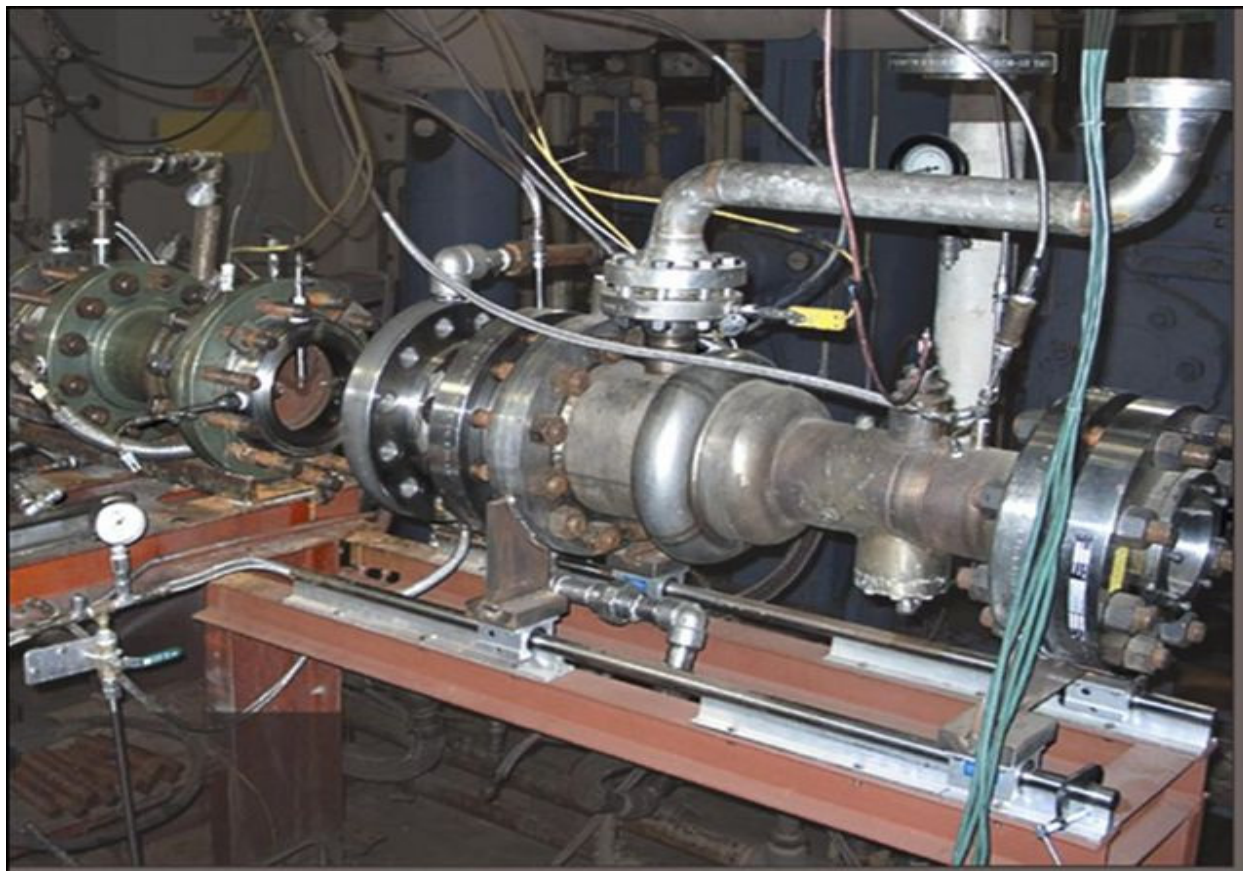


Figure 21.—High Pressure Burner Rig (HPBR). NASA photo C-1996-314, January 1996.

The HPBR is typically used as a materials test rig best suited for testing various sized coupons, bars, and disks of candidate materials, including metals, ceramics, and plasma sprayed coatings. As an example, HPBR data has enabled researchers to make major contributions in our knowledge of advanced materials such as silicon-based monolithic and composite ceramics (Refs. 46 to 48). In these experiments the effects of water vapor and scale volatility were studied on coupon-type test samples to provide oxidation mechanisms. However, complex-shaped components can also be accommodated including cylinders, airfoils, vanes, and film-cooled end walls. Examples of sub-component test samples are found in References 49 and 50. The facility has also been used to evaluate thin-film temperature measurements, microwave sensors, and embedded thermocouples.

http://www.lerc.nasa.gov/WWW/EDB/Facilities/high_pressure_burner_facility.htm

A now defunct natural gas/compressed air burner (Figs. 22 and 23) was used to produce velocities up to Mach 1 and specimen temperatures up to 2000 °F/1093 °C (Refs. 51 to 59). The burner was designed to burn natural gas with compressed air up to approximately 55 psia (0.038 MN/m²) with exit gas temperatures as high as 3000 °F (1649 °C). A double liner was used to permit the combustion air to efficiently cool the outer jacket as well as the flame tube. Water cooling was used only on the converging exit nozzle. Accordingly, heat losses were minimized and the resulting fuel/air ratio was as lean as possible.

The now defunct Hot Corrosion Test Facility (Figs. 24 and 25) - also known as the 4-Atmosphere Burner Rig - at the NASA Lewis Special Projects Laboratory (SPL, or building 24) was a high-velocity, pressurized Mach 0.3 burner rig used to evaluate the hot corrosion of advanced ceramic materials such as silicon carbide and silicon nitride (Refs. 60 to 64). A salt water solution (2 to 5 parts per million) was injected into the burner flame. Maximum air flow was 250 kg/hr (550 lbm/hr), test pressure range was 100 to 600 kPa (1 to 6 atm), and maximum gas temperature exceeded 1500 °C (2732 °F). The test samples in this rig were normally held at 400 kPa (60 psi, or 4 atm) since deposition of salt and subsequent corrosion is a function of total pressure dew point. The rig was dismantled in 2001.

Figures 26 to 30 are a collection of archival photographs.

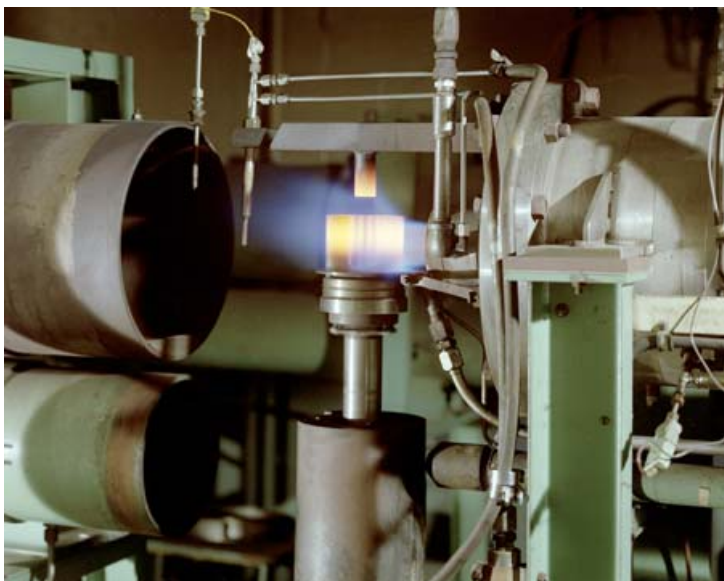


Figure 22.—Mach 1 burner rig. NASA photo C-1969-3870, November 1969.



Figure 23.—Mach 1 burner rig. NASA photo C-1977-1605.

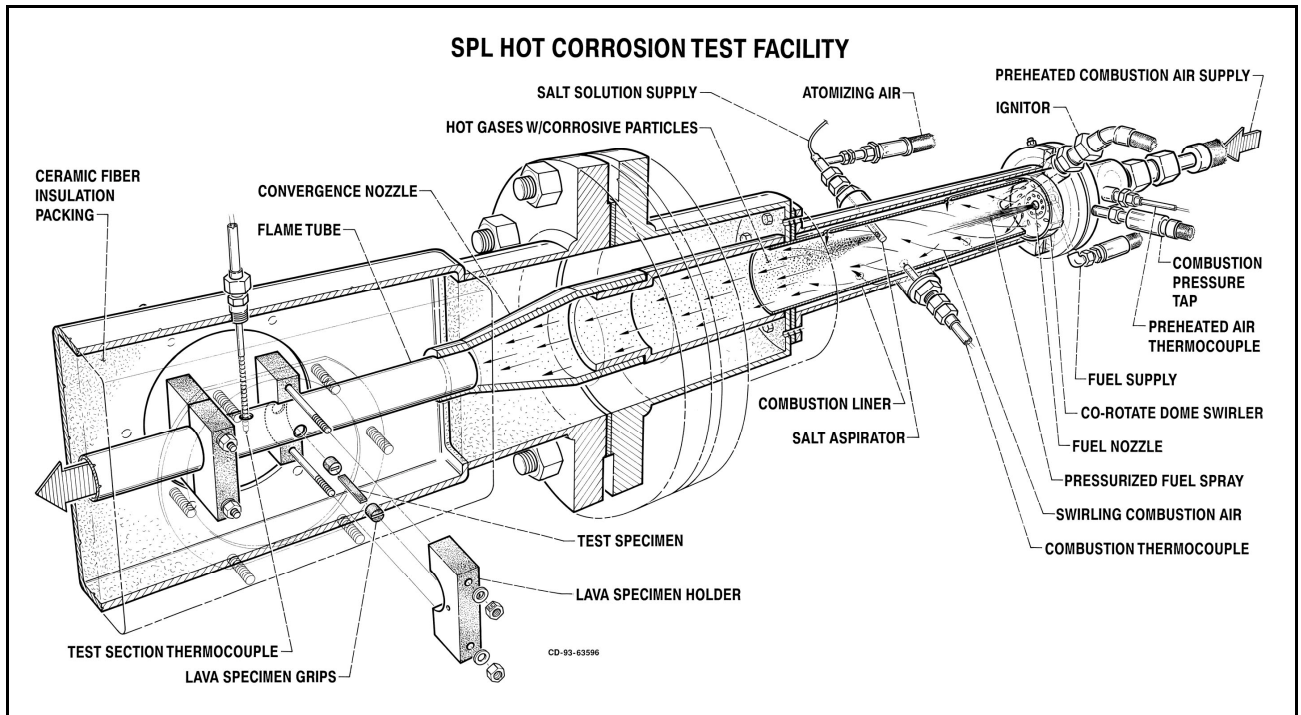


Figure 24.—Cross section drawing of 4-atmosphere corrosion burner rig. (CD-93-63596).

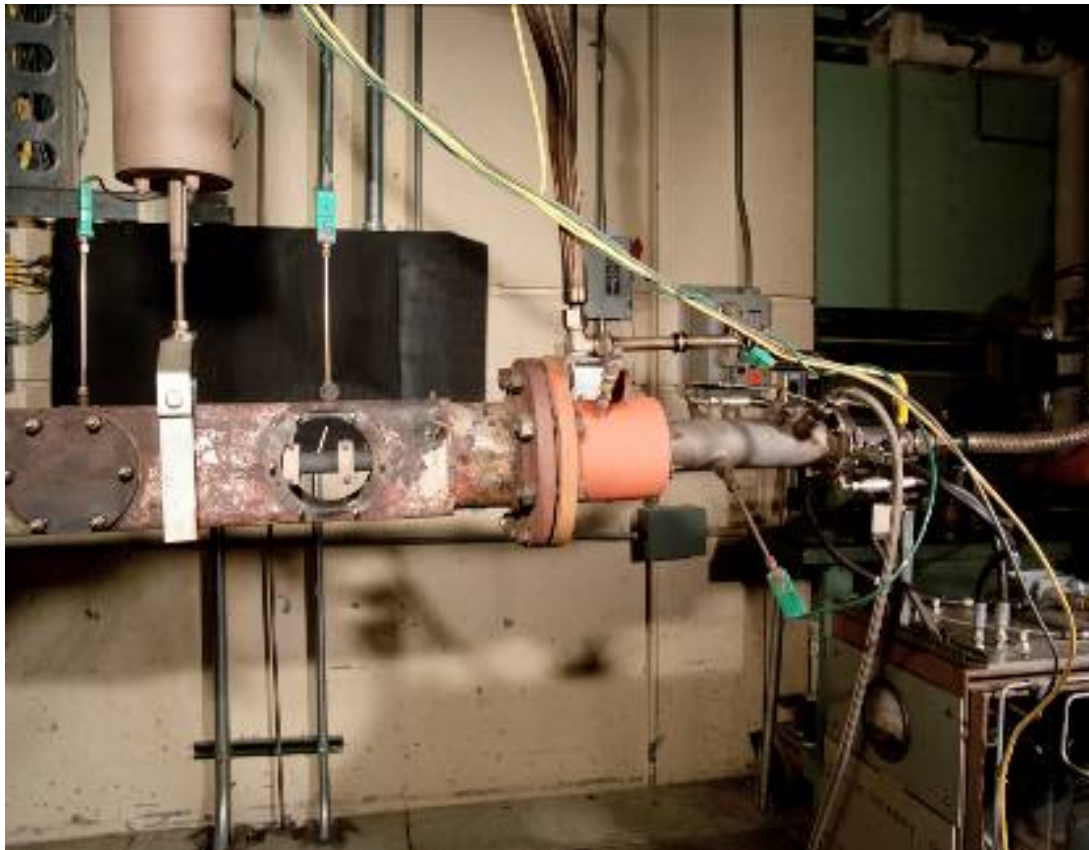


Figure 25.—4-atmosphere corrosion rig circa 1992 (C-92-6666).

Collection of Archival Photographs

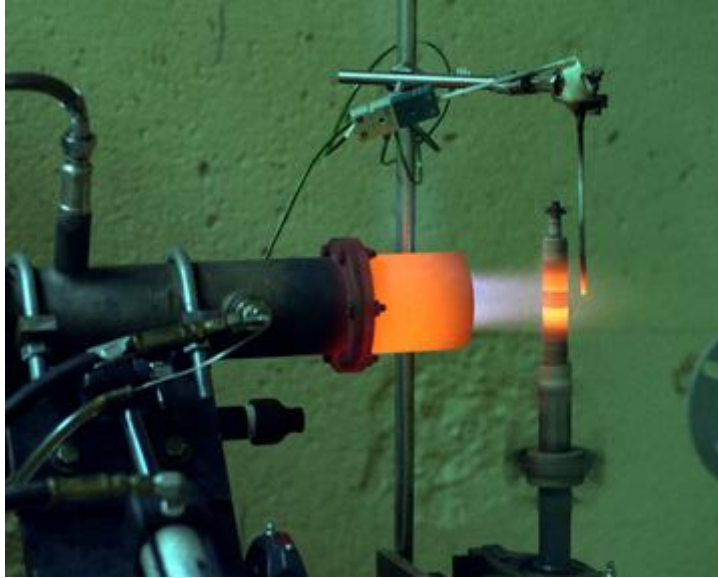


Figure 26.—Mach 0.3 burner rig in operation circa 1979 (C-1979-2390).

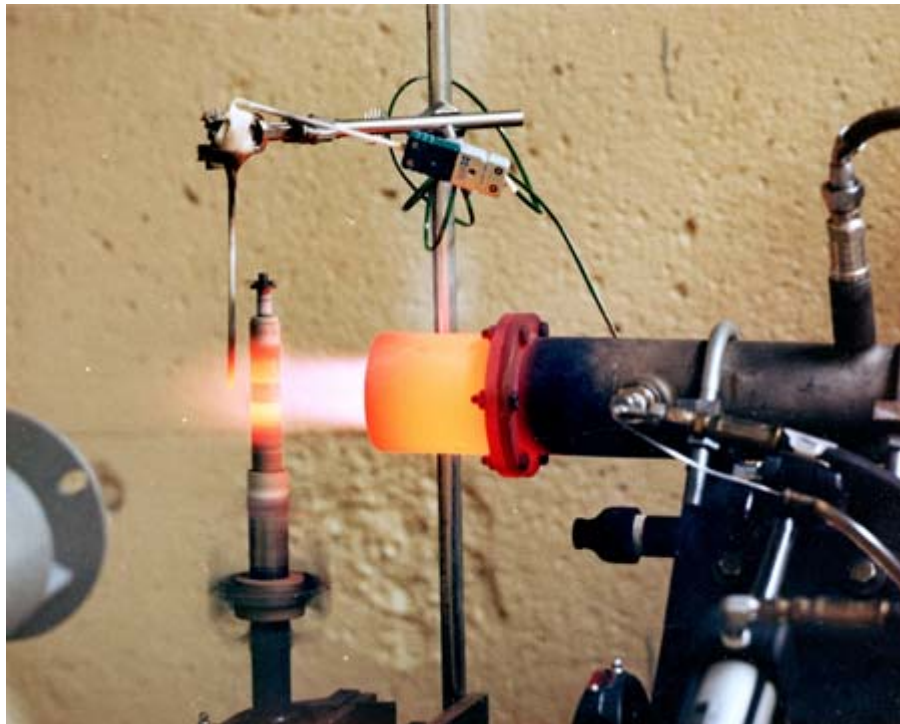


Figure 27.—Mach 0.3 burner rig in operation circa 1982 (C-1982-6121).

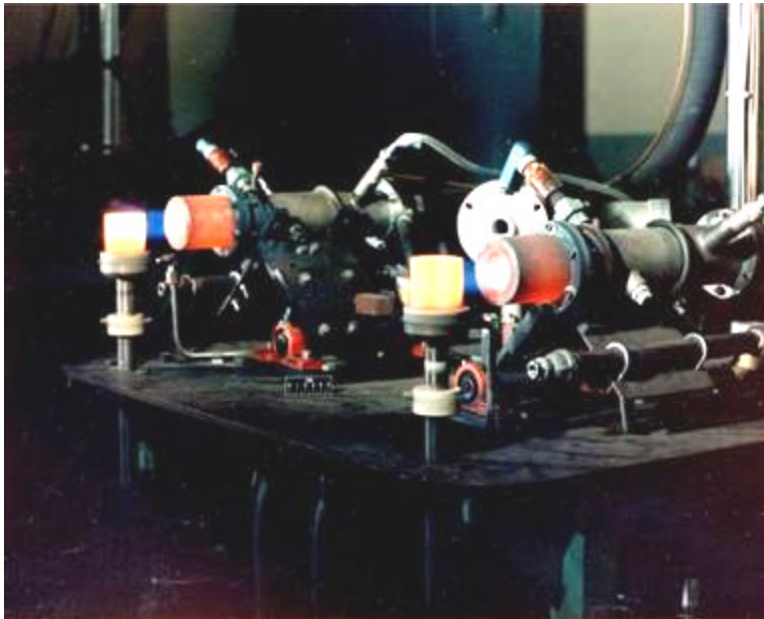


Figure 28.—Mach 0.3 burner rig deposition experiment 1982 (C-1982-6122). Prior to 1985, there were just four Mach 0.3 burner rigs, and they were located in cell 4 of building 24 (Special Projects Laboratory). As shown above, the rigs were in pairs on two different tables. In the course of oxidation and corrosion testing, this arrangement was found to be unsatisfactory in that it allowed “cross-talk” between rigs and skewed experimental results. This is the reason behind each rig being currently housed in its own separate cell in building 34/MRL.

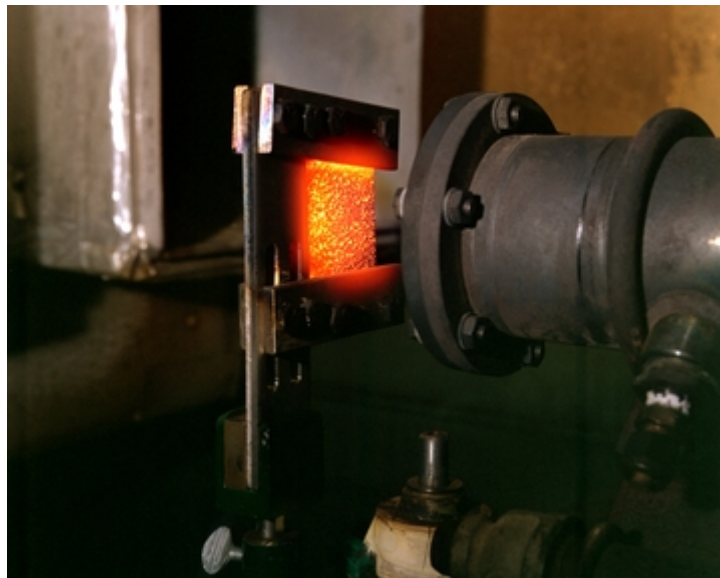


Figure 29.—Oxidation of coated superalloy specimen circa 1986 (C-1986-4728).

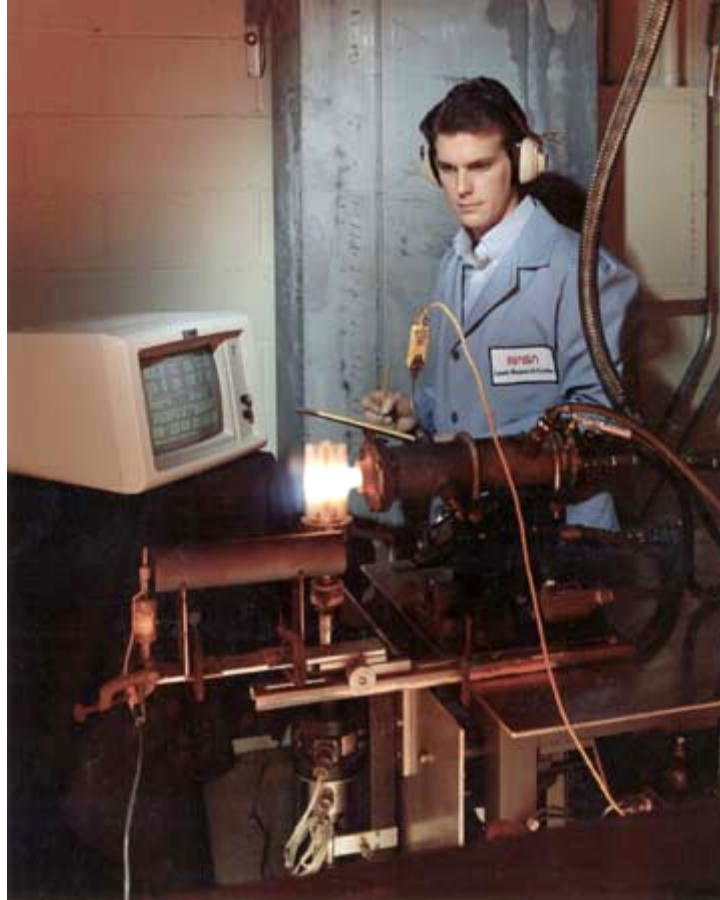


Figure 30.—Burner rig/personal computer publicity photo circa 1990 (C-1990-136).

References

Notes: Beginning with Reference 5, all papers through number 43 relate to historic Mach 0.3 studies and are listed in chronological order. References 44 to 50 relate to the high pressure burner rig. References 51 to 59 relate to the defunct Mach 1 burner rig. References 60 to 64 relate to the defunct 4-atmosphere corrosion burner rig. Also, many of the historic papers in this technical memorandum can be found on the NASA Scientific and Technical website at <http://www.sti.nasa.gov/nasaonly/resrch.html>.

1. Robinson, R.C.; Cuy, M.D., "Hot Corrosion Test Facility at the NASA Lewis Special Projects Laboratory," NASA-CR-195323 May 1, 1994.
2. Deadmore, D.L., "Digital Temperature and Velocity Control of Mach 0.3 Atmospheric Pressure Durability Testing Burner Rigs in Long Time, Unattended Cyclic Testing," NASA TM-86959, March 1, 1985.
3. Rinehart, R.D. and Cuy, M.D., "Mach 0.3 Burner Rig Operator's Manual," Sverdrup Technology, Inc. Contract NAS3-24105, October 7, 1987.
4. Zhu, D., Miller, R.A., and Kuczmariski, M.A., "Development and Life Prediction of Erosion Resistant Turbine Low Conductivity Thermal Barrier Coatings," NASA/TM—2010-215669, February 2010.
5. Lowell, C.E., Deadmore, D.L., "Effect of a Chromium-Containing Fuel Additive on Hot Corrosion," NASA-TM-X-73465, July 1, 1976.

6. Deadmore, D.L. and Lowell, C.E., "Burner Rig Alkali Salt Corrosion of Several High Temperature Alloys." NASA TM-X-73659, May 13, 1977.
7. Lowell, C.E., Deadmore, D.L., "Effect of a Chromium-Containing Fuel Additive on Hot Corrosion," *Corrosion Science*, 18 [8] pp. 747–763, January 1, 1978.
8. Deadmore, D.L., Lowell, C.E., Kohl, F.J., "The Effect of Fuel-To-Air Ratio on Burner-Rig Hot Corrosion," NASA TM-78960, July 1, 1978. Also in *Corrosion Science*, 19, pp. 371–378.
9. Deadmore, D.L., Lowell, C.E., "Inhibition of Hot Salt Corrosion by Metallic Additives," NASA-TM-78966, July 1, 1978.
10. Miller, R.A., "Analysis of the Response of a Thermal Barrier Coating to Sodium and Vanadium Doped Combustion Gases," NASA-TM-79205, January 1, 1979.
11. Deadmore, D.L., Lowell, C.E., "Airfoil Cooling Hole Plugging By Combustion Gas Impurities of The Type Found In Coal Derived Fuels," NASA-TM-79076, February 1, 1979.
12. Hodge, P.E., Miller, R.A., Gedwill, M.A., "Evaluation of Hot Corrosion Behavior of Thermal Barrier Coatings," NASA-TM-81520, January 1, 1980.
13. Lowell, C.E., Sidik, S.M. and Deadmore, D.L., "Effect of Sodium, Potassium, Magnesium, Calcium & Chlorine on High Temperature Corrosion of IN-100, U-700, IN-792 & Mar M-509," NASA TM-79309, January 1, 1980.
14. Deadmore, D.L. and Lowell, C.E., "Effects of Impurities in Coal-Derived Liquids on Accelerated Hot Corrosion of Superalloys," NASA TM-81384, March 1, 1980.
15. Hodge, P.E., Miller, R.A., Gedwill, M.A., "Evaluation of the Hot Corrosion Behavior of Thermal Barrier Coatings," in *Metallurgical coatings 1980*, Proceedings of the Seventh International Conference, San Diego, CA, April 21–25, 1980. Volume 2. (A82-17251 05-23) Lausanne, Elsevier Sequoia, S.A., 1980, pp. 447–453.
16. Santoro, G.J., Kohl, F.J., Stearns, C.A., Fryburg, G.C., Johnson, J.R., "Deposition and Material Response From Mach 0.3 Burner Rig Combustion of SRC 2 Fuels," NASA-TM-81634, October 1, 1980.
17. Levine, S.R., Miller, R.A., Hodge, P.E., "Thermal Barrier Coatings for Heat Engine Components," *SAMPE Quarterly*, 12, October, 1980, pp. 20–26.
18. Lowell, C.E., Deadmore, D.L., Santoro, G.J., Kohl, F.J., "The Effects of Trace Impurities in Coal-Derived Liquid Fuels on Deposition and Accelerated High Temperature Corrosion of Cast Superalloys," NASA TM-81678, January 1, 1981.
19. Hodge, P.E., Miller, R.A., Gedwill, M.A., Zaplatynsky, I., "Review of NASA Progress in Thermal Barrier Coatings for Stationary Gas Turbines," NASA-TM-81716 January 1, 1981.
20. Lowell, C.E., Sidik, S.M., Deadmore, D.L., "High Temperature Alkali Corrosion in High Velocity Gases," NASA-TM-82591, May 1, 1981.
21. Miller, R.A., Lowell, C.E., "Failure Mechanisms of Thermal Barrier Coatings Exposed To Elevated Temperatures," NASA-TM-82905, January 1, 1982.
22. Lowell, C.E., Deadmore, D.L., Whittenberger, J.D., "Long-Term High-Velocity Oxidation and Hot Corrosion Testing of Several NiCrAl and FeCrAl Base Oxide Dispersion Strengthened Alloys," *Oxidation of Metals*, vol. 17, pp. 205–221, April, 1982.
23. Levine, S.R., Miller, R.A., "Thermal-Barrier Coatings for Utility Gas Turbines," NASA TM-85349, September 1, 1982.
24. Deadmore, D.L., Lowell, C.E. Burner Rig Study of Variables Involved in Hole Plugging of Air Cooled Turbine Engine Vanes," NASA-TM-83308, February 1, 1983.
25. Santoro, G.J., Gokoglu, S.A., Kohl, F.J., Stearns, C.A., Rosner, D.E., "Deposition of Na₂SO₄ From Salt-Seeded Combustion Gases of a High Velocity Burner Rig," NASA-TM-83751, January 1, 1984.
26. Deadmore, D.L., "Application of Induction Coil Measurements to the Study of Superalloy Hot Corrosion and Oxidation," NASA-TM-83560, January 1, 1984.
27. Santoro, G.J., Kohl, F.J., Stearns, C.A., Gokoglu, S.A., Rosner, D.E., "Experimental and Theoretical Deposition Rates from Salt-Seeded Combustion Gases of a Mach 0.3 Burner Rig," NASA-TP-2225, March 1, 1984.

28. Deadmore, D.L., "In-Situ Measurements of Alloy Oxidation/Corrosion/Erosion Using a Video Camera & Proximity Sensor with Microcomputer Control," NASA TM-83673, May 1984.
29. Deadmore, D.L., "Effects of Alloy Composition on Cyclic Flame Hot-Corrosion Attack of Cast Nickel-Base Superalloys at 900 °C," NASA TP-2338, July 1, 1984.
30. Stearns, C.A., Deadmore, D.L., Barrett, C.A. Effect of Alloy Composition on the Sodium-Sulfate Induced Hot Corrosion Attack of Cast Nickel-Base Superalloys at 900 °C," in the proceedings of Alternate Alloying for Environmental Resistance, held in New Orleans, LA, Mar. 2–6, 1986. Warrendale, PA, Metallurgical Society, Inc., 1987, pp. 131–143.
31. Brindley, W.J., Miller, R.A., "Thermal Barrier Coating Life And Isothermal Oxidation of Low-Pressure Plasma-Sprayed Bond Coat Alloys," in *Metallurgical Coatings and Thin Films 1990*, Proceedings of the 17th International Conference on Metallurgical Coatings and 8th International Conference on Thin Films, San Diego, CA, April 2–6, 1990. vol. 1 (A92-32376 12-23). London and New York, Elsevier Applied Science, 1990, pp. 446–457.
32. Lei, J-F, Cuy, M.D., Wnuk, S.P., "Attachment of Free Filament Thermocouples for Temperature Measurements on CMC," NASA TM-107488, June 1997.
33. Enabling Propulsion Materials Program Annual Technical Progress Report, Volume 3: Task B – Exhaust Nozzle, pp. 142–145. January 31, 1998.
34. Nesbitt, James A., "Hot Corrosion of Single-Crystal NiAl-X Alloys," NASA TM 113128, May 1998.
35. Nesbitt, James A., Darolia, Ram, Cuy, Michael D., "Burner Rig Hot Corrosion of a Single Crystal Ni-48Al-Ti-Hf-Ga Alloy," *Mat. Res. Soc. Symp. Proc.* vol. 522, pp. KK9.5.1 to 9.5.6, The Materials Research Society, 1999.
36. Lei, J-F, Kiser, J.D., Singh, M. Cuy, M.D. Blaha, C.A., Androjna, D., "Durability Evaluation of a Thin Film Sensor System with Enhanced Lead Wire Attachments on SiC/SiC Ceramic Matrix Composites," NASA/TM—2000-209917, March 2000.
37. Nesbitt, James A., Harris, K., Helmink, R., and Erickson, G., "Burner Rig Hot Corrosion of Five Ni-Base Alloys Including Mar-M247," Published in *Corrosion 2001*, pp. 01166/1-14, NACE International, Houston, TX (2001).
38. Opila, E.J., Robinson, Raymond C., Cuy, Michael D., "High Temperature Corrosion of Silicon Carbide and Silicon Nitride in Water Vapor," 10th International Conferences on Modern Materials and Technologies (CIMTEC 2002).
39. Zhu, Dongming, Kuczmariski, Maria A., Miller, Robert A., Cuy, Michael D., "Evaluation of Erosion Resistance of Advanced Turbine Thermal Barrier Coatings," January 22, 2007. 31st International Cocoa Beach Conference & Exposition on Advanced Ceramics and Composites, Daytona Beach, FL.
40. Bhatt, R.T., Choi, S.R., Cosgriff, L.M., Fox, D.S., Lee, K.N., "Impact resistance of environmental barrier coated SiC/SiC composites," *Materials Science and Engineering A* 476 (2008) 8–19.
41. Bhatt, R.T., Choi, S.R., Cosgriff, L.M., Fox, D.S., Lee, K.N., "Impact resistance of uncoated SiC/SiC composites," *Materials Science and Engineering A* 476 (2008) 20–28.
42. *Dongming Zhu, Robert A. Miller, and Maria A. Kuczmariski*, "Development and Life Prediction of Erosion Resistant Turbine Low Conductivity Thermal Barrier Coatings," NASA/TM—2010-215669, February 2010.
43. M.B. Beardsley, "Thick thermal barrier coatings for diesel engines," *Journal of Thermal Spray Technology* vol. 6 [2] 181-186 June 1997.
44. Stearns, C.A. and Robinson, R.C, "NASA Lewis Research Center Lean-, Rich-Burn Materials Test Burner Rig," NASA CR 194437, February 1994.
45. Robinson, R. Craig, "NASA GRC's High Pressure Burner Rig Facility and Materials Test Capabilities," NASA/CR 19990209411, December 1999.
46. Smialek, J.L., Robinson, R.C., Opila, E.J., Fox, D.S., Jacobson, Nathan S., "SiC and Si₃N₄ Recession Due to SiO₂ Scale Volatility under Combustor Conditions," NASA/TP-1999-208696, July 1999.
47. R.C. Robinson and J.L. Smialek, "SiC Recession Caused by SiO₂ Scale Volatility under Combustion Conditions. Part I: Experimental Results and Empirical Model," *J. Am. Ceram. Soc.*, 82 [7] 1817-25 (1999).

48. E.J. Opila, J.L. Smialek, R.C. Robinson, D.S. Fox, and N.S. Jacobson, "SiC Recession Caused by SiO₂ Scale Volatility under Combustion Conditions. Part II: Thermodynamics and Gaseous Diffusion Model," *J. Am. Ceram. Soc.*, 82 [7] 1826-34 (1999).
49. R.C. Robinson and K.S. Hatton, "SiC/SiC Leading Edge Turbine Airfoil Tested Under Simulated Gas Turbine Conditions," NASA/CR-1999-209314, September 1999.
50. Zhu, Dongming; Fox, Dennis S.; Pastel, Robert T., "High Pressure Burner Rig Testing of Advanced Environmental Barrier Coatings for Si₃N₄ Turbine Components," 31st International Cocoa Beach Conference & Exposition on Advanced Ceramics & Composites, 22–26 January. 2007, Daytona Beach, FL.
51. Ashbrook, R.L.; Johnston, J.R., "Oxidation and Thermal Fatigue Cracking of Nickel- and Cobalt-base Alloys in a High Velocity Gas Stream," NASA-TN-D-5376, August 1969.
52. Deadmore, D.L.; Grisaffe, S.J.; Sanders, W.A., "Furnace and High-Velocity Oxidation of Aluminide-Coated Cobalt Super-Alloy WI-52." NASA TN-D-5834, May 1970.
53. Deadmore, D.L., "Cyclic Oxidation of Cobalt-Chromium-Aluminum-Yttrium and Aluminide Coatings on IN-100 and VIA Alloys in High Velocity Gases," NASA TN-D-6842, July 1972.
54. Deadmore, D.L., "High-Velocity-Oxidation Performance of Metal-Chromium-Aluminum (MCrAl), Cermet, And Modified Aluminide Coatings on IN-100 and type VIA alloys at 1093 C," NASA TN-D-7530, February 1974.
55. Deadmore, D.L.; Lowell, C.E., "High Gas Velocity Oxidation and Hot Corrosion Testing of Oxide Dispersion-Strengthened Nickel-Base Alloys," NASA-TM-X-71835, November 1, 1975.
56. Lowell, C.E.; Deadmore, D.L., "High Velocity Oxidation and Hot Corrosion Resistance of Some ODS Alloys." NASA TM-X-73656, April 1, 1977.
57. Sanders, William A., Johnston, James R., "High Velocity Burner Rig Oxidation and Thermal Fatigue Behavior of Si₃N₄- and SiC-based Ceramics to 1370 °C," NASA TM-79040, November, 1978.
58. Young, S.G. and Deadmore, D.L., "An Experimental, Low-Cost, Silicon Slurry/Aluminide High-Temperature Coating For Superalloys," NASA TM-79178, July 1979.
59. Young, S.G. and Deadmore, D.L., "An Experimental, Low-Cost, Silicon-Aluminide High-Temperature Coating For Superalloys," NASA TM-81455, January, 1980.
60. Robinson, R.C.; Cuy, M.D., "Hot Corrosion Test Facility at the NASA Lewis Special Projects Laboratory," NASA-CR-195323 May 1, 1994.
61. Jacobson, N.S.; Stearns, C.A.; Smialek, J.L., "Burner rig corrosion of SiC at 1000 °C," *Advanced Ceramic Materials*, vol. 1, April 1986, pp. 154–161.
62. Fox, D.S. and Smialek, J.L., "Burner Rig Hot Corrosion of Silicon Carbide and Silicon Nitride," *J. Am. Ceram. Soc.*, 73 [2] 303-11 (1990).
63. Fox, D.S., Cuy, M.D. and Strangman, T.E., "Sea Salt Hot Corrosion and Strength of a Yttria-Containing Silicon Nitride," *J. Am. Ceram. Soc.* 80 [11] 2798-804 (1997).
64. Fox, D.S., Cuy, M.D., and Nguyen, Q.N., "Sea Salt Hot Corrosion of a Sintered α-Silicon Carbide," *J. Am. Ceram. Soc.*, 81 [6] 1565-70 (1998).

REPORT DOCUMENTATION PAGE			Form Approved OMB No. 0704-0188		
<p>The public reporting burden for this collection of information is estimated to average 1 hour per response, including the time for reviewing instructions, searching existing data sources, gathering and maintaining the data needed, and completing and reviewing the collection of information. Send comments regarding this burden estimate or any other aspect of this collection of information, including suggestions for reducing this burden, to Department of Defense, Washington Headquarters Services, Directorate for Information Operations and Reports (0704-0188), 1215 Jefferson Davis Highway, Suite 1204, Arlington, VA 22202-4302. Respondents should be aware that notwithstanding any other provision of law, no person shall be subject to any penalty for failing to comply with a collection of information if it does not display a currently valid OMB control number.</p> <p>PLEASE DO NOT RETURN YOUR FORM TO THE ABOVE ADDRESS.</p>					
1. REPORT DATE (DD-MM-YYYY) 01-03-2011		2. REPORT TYPE Technical Memorandum		3. DATES COVERED (From - To)	
4. TITLE AND SUBTITLE Mach 0.3 Burner Rig Facility at the NASA Glenn Materials Research Laboratory			5a. CONTRACT NUMBER		
			5b. GRANT NUMBER		
			5c. PROGRAM ELEMENT NUMBER		
6. AUTHOR(S) Fox, Dennis, S.; Miller, Robert, A.; Zhu, Dongming; Perez, Michael; Cuy, Michael, D.; Robinson, R., Craig			5d. PROJECT NUMBER		
			5e. TASK NUMBER		
			5f. WORK UNIT NUMBER WBS 031102.02.03.0676.09		
7. PERFORMING ORGANIZATION NAME(S) AND ADDRESS(ES) National Aeronautics and Space Administration John H. Glenn Research Center at Lewis Field Cleveland, Ohio 44135-3191			8. PERFORMING ORGANIZATION REPORT NUMBER E-17628		
9. SPONSORING/MONITORING AGENCY NAME(S) AND ADDRESS(ES) National Aeronautics and Space Administration Washington, DC 20546-0001			10. SPONSORING/MONITOR'S ACRONYM(S) NASA		
			11. SPONSORING/MONITORING REPORT NUMBER NASA/TM-2011-216986		
12. DISTRIBUTION/AVAILABILITY STATEMENT Unclassified-Unlimited Subject Categories: 26 and 27 Available electronically at http://www.sti.nasa.gov This publication is available from the NASA Center for AeroSpace Information, 443-757-5802					
13. SUPPLEMENTARY NOTES					
14. ABSTRACT This Technical Memorandum presents the current capabilities of the state-of-the-art Mach 0.3 Burner Rig Facility. It is used for materials research including oxidation, corrosion, erosion and impact. Consisting of seven computer controlled jet-fueled combustors in individual test cells, these relatively small rigs burn just 2 to 3 gal of jet fuel per hour. The rigs are used as an efficient means of subjecting potential aircraft engine/airframe advanced materials to the high temperatures, high velocities and thermal cycling closely approximating actual operating environments. Materials of various geometries and compositions can be evaluated at temperatures from 700 to 2400 °F. Tests are conducted not only on bare superalloys and ceramics, but also to study the behavior and durability of protective coatings applied to those materials.					
15. SUBJECT TERMS High temperature; Degradation; Oxidation; Corrosion					
16. SECURITY CLASSIFICATION OF:			17. LIMITATION OF ABSTRACT	18. NUMBER OF PAGES 33	19a. NAME OF RESPONSIBLE PERSON STI Help Desk (email:help@sti.nasa.gov)
a. REPORT U	b. ABSTRACT U	c. THIS PAGE U			19b. TELEPHONE NUMBER (include area code) 443-757-5802

